One-dimensional nanostructures for electronic and optoelectronic devices

Guozhen SHEN (✉), Di CHEN

Wuhan National Laboratory for Optoelectronics, College of Optoelectronic Science and Engineering,
Huazhong University of Science and Technology, Wuhan 430074, China

Abstract One-dimensional (1-D) nanostructures have been the focus of current researches due to their unique physical properties and potential applications in nanoscale electronics and optoelectronics. They address and overcome the physical and economic limits of current microelectronic industry and will lead to reduced power consumption and largely increased device speed in next generation electronics and optoelectronics. This paper reviews the recent development on the device applications of 1-D nanostructures in electronics and optoelectronics. First, typical 1-D nanostructure forms, including nanorods, nanowires, nanotubes, nanobelts, and hetero-nanowires, synthesized from different methods are briefly discussed. Then, some nanoscale electronic and optoelectronic devices built on 1-D nanostructures are presented, including field-effect transistors (FETs), p-n diodes, ultraviolet (UV) detectors, light-emitting diodes (LEDs), nanolasers, integrated nanodevices, single nanowire solar cells, chemical sensors, biosensors, and nanogenerators. We then finalize the paper with some perspectives and outlook towards the fast-growing topics.

1 Introduction

The development of microelectronic industry greatly improves human beings' lives, and the rapid miniaturization of electronics to the submicron scale has led to remarkable advances in computing power and reducing costs. However, the physical and economic limits of current microelectronic industry will be soon reached as it advances towards ever smaller devices since the most

commonly used technique in microelectronic industry is so-called top-down strategies, which have both resolution limit and cost problem. Bottom-up technology was then developed as a much powerful strategy to meet the expected demand for increased power consumption and reducing costs. The bottom-up method could produce high-quality one-dimensional (1-D) nanostructure building blocks with controlled compositions, doping states, diameters, and lengths, and thus enable entirely new device concepts and new systems [1–3].

1-D nanostructures represent the smallest dimension structure that can efficiently transport electrical carriers. They can be rationally synthesized in a single crystal form with controlled key parameters during growth, such as chemical composition, doping state, diameter, length, etc. Till now, 1-D nanostructures, nanowires, nanotubes, nanorods, nanobelts, nanorings, and hetero-nanowires can be produced for a host of materials, including semiconductors, metals, and polymers, by using techniques like solution methods, template-assisted methods, vapor phases methods, etc. [4–53]. The ability to produce 1-D nanostructures with controlled key parameters makes it possible to fabricate functional nanoscale devices [1–3,5,6,26–29]. For example, 1-D nanostructures have been assembled into nanoscale field-effect transistors (FETs), p-n diodes, ultraviolet (UV) detectors, light-emitting diodes (LEDs), nanolasers, integrated nanowire devices, single nanowire solar cells, chemical sensors, biosensors, and nanogenerators.

This paper reviews the state-of-the-art research activities in 1-D nanostructure-based electronic and optoelectronic devices and can be divided into three main sections. The first part briefly introduces 1-D nanostructure forms, including nanorods, nanowires, nanotubes, nanobelts, and hetero-nanowires, each with one or two examples, synthesized from different methods. Then, some typical nanoscale electronic and optoelectronic devices built on 1-D nanostructures are presented, including FETs, p-n

diodes, UV detectors, LEDs, nanolasers, integrated nanodevices, single nanowire solar cells, chemical sensors, biosensors, and nanogenerators. At last, some perspectives and outlook towards the fast-growing topics will be discussed.

2　1-D nanostructure forms

There are many forms of 1-D nanostructures, including nanorods, nanowires, nanotubes, nanobelts, and hetero-nanowires, which are usually categorized by their aspect ratios, cross-sections, or compositions as illustrated in Fig. 1.
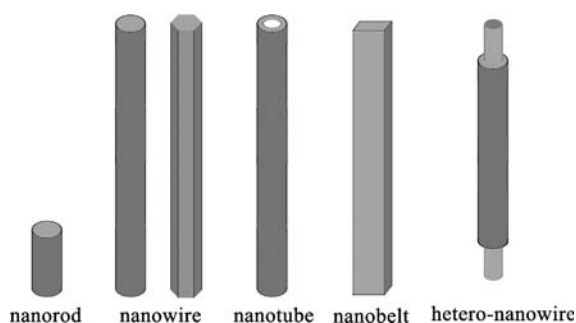

Fig. 1　Typical forms of 1-D nanostructures

2.1　Nanorods

1-D nanostructures with aspect ratios less than 10 are generally discriminated as nanorods [54–56]. Solution methods are the most powerful techniques to synthesize nanorods with different compositions. Figure 2(a) shows a scanning electron microscopy (SEM) image of ordered Au nanorods assemblies formed by an interesting droplet evaporation method [54]. In this process, Au nanorods were first prepared using a seeded growth method with ammonium surfactants as stabilizing agents. After treated, droplets of Au nanorods were evaporated to get the ordered assemblies. Figure 2(b) is the transmission electron microscopy (TEM) image of some aligned Au nanorods with lengths of around 200 nm [55]. The diameters of these nanorods are quite uniform of about 20 nm.

2.2　Nanowires

In contrast to nanorods, 1-D nanostructures with aspect ratios larger than 10 are usually described as nanowires [4,29–31]. Nanowires have been produced for many materials by using different methods. The developed synthetic methods include chemical vapor deposition (CVD), solution methods, template-assisted methods, and some special ones [10–50]. Figure 3(a) shows the SEM image of In_2O_3 nanowires synthesized from a laser ablation CVD method. In this method, InAs was used as
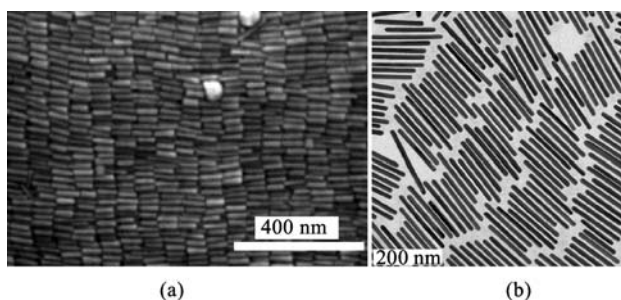

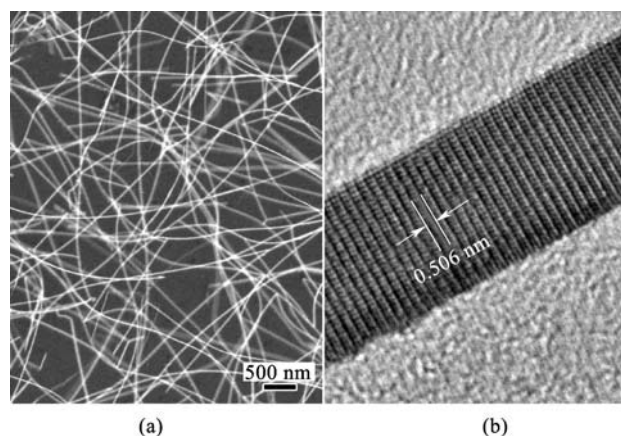**Fig. 2**　(a) SEM and (b) TEM images of Au nanorods (Reprinted with permission from Refs. [54,55])

Fig. 3　(a) SEM and (b) HRTEM images of In_2O_3 nanowires synthesized from laser ablation CVD method

the target, and Au-coated Si substrate was used to deposit the final product. From this image, it can be clearly seen that long In_2O_3 nanowires were synthesized on a large scale. Typical nanowires have diameters of ca. 10–20 nm with lengths of several tens of micrometers. A high-resolution TEM (HRTEM) image of a single In_2O_3 nanowire is illustrated in Fig. 3(b), which indicates the single crystal nature of the nanowire. The clearly resolved lattice fringe in this image is around 0.506 nm, corresponding to the (100) plane of cubic In_2O_3 phase. These nanowires have the preferred growth directions along the [010] orientations.

Among solution methods, the solvothermal method, which was performed in a sealed autoclave, provides a much powerful approach to synthesize semiconductor nanowires. Figure 4 is a SEM image of long CdS nanowires produced from the solvothermal method. In this process, Cd substrate and S powder were used as the source materials and ethylenediamine as the solvent. After reaction, CdS nanowires were grown on the whole substrate. These nanowires are single crystals with wurtzite structure. The growth direction is the [001] orientation. During the solvothermal process, the source materials, the solvent, temperature, and surfactant have great influence
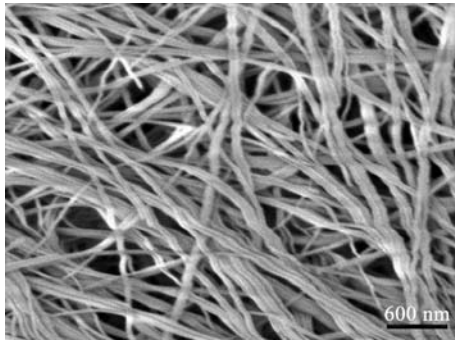
Fig. 4 SEM image of CdS nanowires produced from solvothermal method

(a)   (b)

Fig. 5 (a) SEM and (b) TEM images of Cd_3P_2 nanotubes by using *in situ* formed Cd nanowires as a sacrificing template

on the morphology of the product. For example, during the above process, if S was substituted by thiourea, only CdS nanoplates are produced on the substrate instead of nanowires.

Though template-assisted method is well developed to synthesize nanowires, the nanowires produced are usually of poor crystallinity or of polycrystalline states. They are not suitable for the fabrications of electronic or optoelectronic devices [52,53].

2.3 Nanotubes

Nanotubes are basically nanowire or nanorod-like structures with hollow channels throughout their lengths. Since the first report on carbon nanotubes by Iijima in 1991, great interests have been paid to inorganic nanotubes with hollow cavities [57].

Nanotubes can be directly synthesized for the materials with layered or pseudo-layered structure. For example, transition metal chalcogenide (MoS_2, $MoSe_2$, WS_2, etc.), $NiCl_2$, BN, and vanadium oxide were directly synthesized using either solution or vapor phase methods [58–65]. For the materials without layered structures, templates, either soft or hard template, or surfactants are usually required to direct the growth of nanotubes. Good examples for the template-assisted synthesized nanotubes are the II-V group semiconducting nanotubes [25]. We developed an *in situ* nanowire template method to synthesize both Zn_3P_2 and Cd_3P_2 nanotubes. In this process, the *in situ* produced nanowires are low melting point Zn or Cd nanowires. In the reaction chamber, the newly produced P gases reacted with the Zn or Cd nanowires to form Zn/Zn_3P_2 or Cd/Cd_3P_2 core/shell nanowires. Once completely consumed, hollow Zn_3P_2 or Cd_3P_2 nanotubes were formed. Figure 5 shows the SEM and TEM images of the synthesized Cd_3P_2 product. The clear brightness contrast indicates their hollow structure. These nanotubes have very thin walls in the range of several to tens of nanometers and open tips. Both Zn_3P_2 and Cd_3P_2 nanotubes are single crystals with the preferred growth directions perpendicular to the (101)
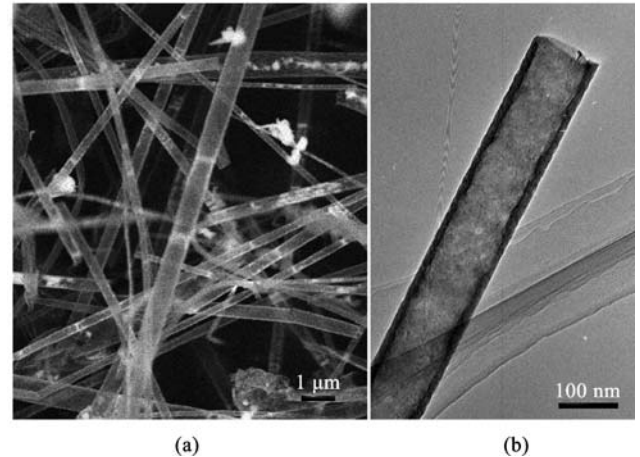
planes. With thin wall thickness, these nanotubes are expected to show size quantization effects.

2.4 Nanobelts

Nanobelts were first discovered for metal oxides by Wang [11]. In nanobelts, the thickness of the belt is much smaller than its width, such that the confinement is far from uniform in the cross section as compared to the above discussed nanowires. The unique structure of nanobelts may help to extend our understanding of structure-property relationships in solids, and it also contributes to an ideal system for building functional electronic and optoelectronic devices.

Since its discovery, several techniques have been developed to get nanobelts, including chemical or physical vapor deposition, hydrothermal or solvothermal growth, and so on [4,7,11,66,67]. Figure 6 shows a series of SEM and TEM images of some nanobelts synthesized from different methods. Figure 6(a) shows the SEM image of $Ag_2V_4O_{11}$ nanobelts synthesized from hydrothermal methods at 180°C. Figure 6(b) shows the Si_3N_4 nanobelts produced by thermal evaporating SiO in N_2 gas at high temperature. Single-crystalline GaS nanobelts were also synthesized using the CVD method as shown in Fig. 6(c). Figure 6(d) shows the TEM image of a single Ag_2WO_4 nanobelt synthesized in a hydrothermal process. All these nanobelts can be produced on a very large scale.

2.5 Hetero-nanowires

Very recently, 1-D hetero-nanowires with modulated compositions and interfaces have become of particular interest due to their potential applications as nanoscale building blocks for future electronic and optoelectronic devices and systems [36,38–42]. The formation of well-defined heterojunctions between different 1-D nanomate-
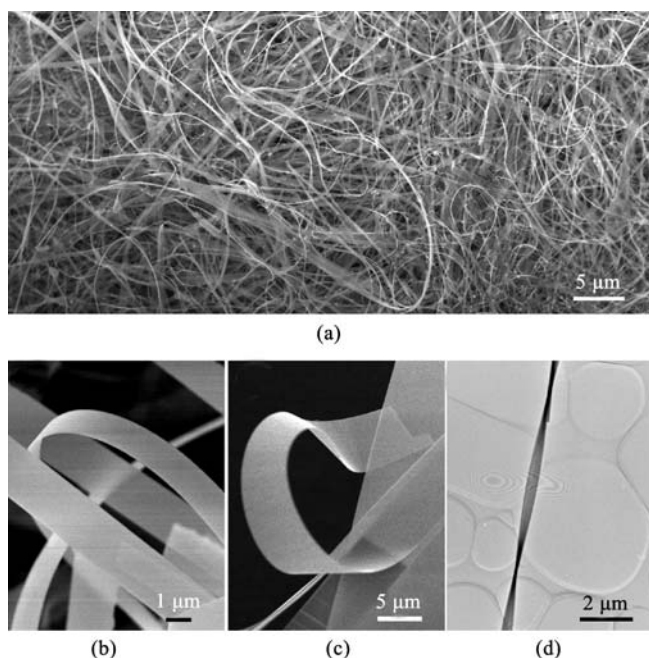
Fig. 6 (a) SEM image of hydrothermally synthesized $Ag_2V_4O_{11}$ nanobelts; (b) SEM image of CVD-produced Si_3N_4 nanobelts; (c) SEM image of CVD-produced GaS nanobelts; (d) TEM image of Ag_2WO_4 nanobelts

rials has led to unique properties that can not be realized in single-component nanostructures. Generally, hetero-nanowires can be classified into three types based on the nature of the junctions within the structure. They are co-axial core/shell, segmented, and hierarchical hetero-nanowires.

Co-axial core/shell hetero-nanowires with different core/shell composition structures are one of the most important categories of hetero-nanowires. The simplest one is the assembly of a nanowire as the core and a nanotube as the shell as shown in Fig. 7(a) [10]. Core/shell Ge/ZnS hetero-nanowires were synthesized by thermal evaporating Ge and ZnS powders. The brightness contrast between the core and the shell gives direct evidence for the formation of core/shell nanostructures. An HRTEM image shown in Fig. 7(b) depicted the resolved lattice fringes of 0.33 nm for both the Ge core and the ZnS shell, in consistent with the (111) plane of cubic Ge phase and the (100) plane of hexagonal ZnS phase, respectively. The interface between the Ge and ZnS is perfect due to the perfect lattice match between cubic Ge and hexagonal ZnS.

Segmented hetero-nanowires, sometimes called super-latticed nanowires, represent another group of interesting hetero-nanowires and have become the forefront of recent research. Figure 7(c) shows SEM images and TEM images
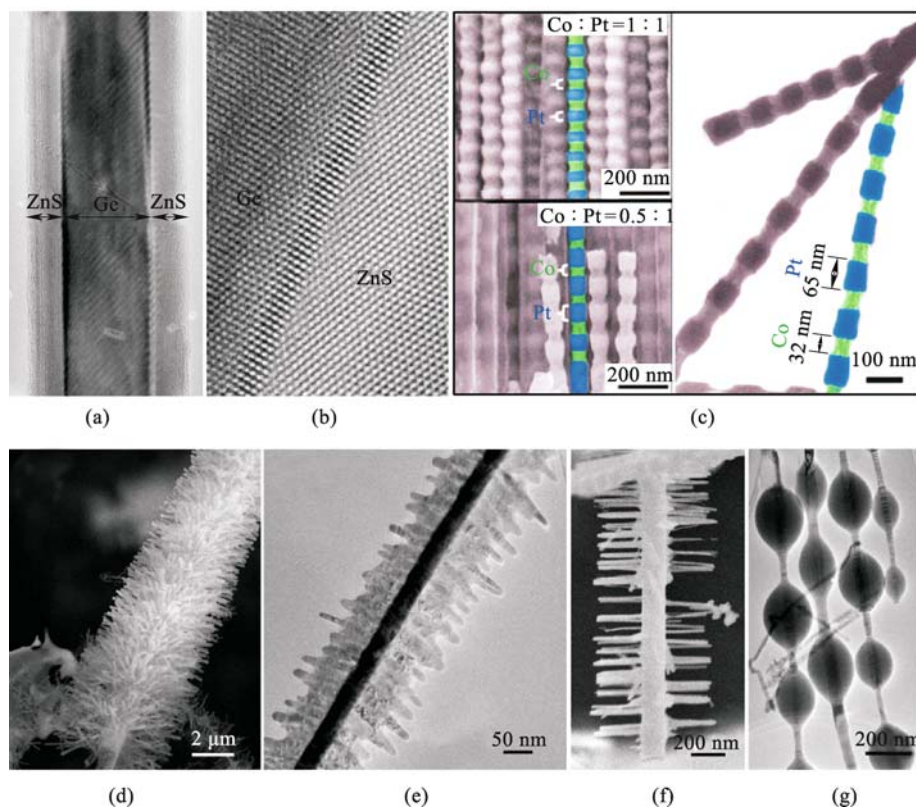

Fig. 7 (a) TEM and (b) HRTEM images of core/shell Ge/ZnS hetero-nanowires; (c) SEM and TEM images of Co/Pt segmented hetero-nanowires; (d)–(g) SEM and TEM images of hierarchical hetero-nanowires (Figure 7(c) was reprinted with permission from Ref. [68])

of segmented Co/Pt hetero-nanowires synthesized by using porous alumina templates in an electrodeposition process [68]. Small Co and Pt segments are arranged periodically along the hetero-nanowires. The lengths of the segments can be easily controlled by tuning the programmable deposition conditions.

Hierarchical assembly of 1-D nanostructures into hierarchical hetero-nanowires is a crucial step towards the realization of functional nanosystems. Figures 7(d)–7(g) show the SEM and TEM images of hierarchical hetero-nanowires with different compositions produced in our group. Figure 7(d) shows the hierarchical C microtube/SiO$_2$ nanowires hetero-nanowires, which are composed of numerous small SiO$_2$ nanowires wrapped around a C microtube. Other hetero-nanowires shown here are hierarchical ZnO nanowire/ZnS nanowire hetero-nanowires where many small ZnS nanowires are grown on a single ZnO nanowire (Fig. 7(e)), hierarchical Zn$_3$P$_2$ nanobelt/ZnS nanowire hetero-nanowires where numerous ZnS nanowires are grown on both sides of a Zn$_3$P$_2$ nanobelt (Fig. 7(f)), and pearl-like ZnS decorated InP hetero-nanowires (Fig. 7(g)).

Hierarchical hetero-nanowires represent a group of complex nanostructures, and they have great potential in electronic and optoelectronic devices. For example, the pearl-like ZnS decorated InP hetero-nanowires show p-type semiconducting behaviors and are sensitive to UV irradiation, which may be used as UV detectors.

3　Nanoscale electronic and optoelectronic devices

The ability to produce 1-D nanostructures with controlled compositions, morphologies, and doping states makes it possible to fabricate nanoscale electronic and optoelectronic devices. Here, a survey on typical nanoscale electronic and optoelectronic devices built on 1-D nanostructures will be given [20–53].

3.1　Field-effect transistors (FETs)

1-D nanostructures can be assembled into FETs. The basic FET structure built on 1-D nanostructures is shown in Fig. 8. In a typical FET, p-type silicon, acting as the back gate, with a layer of SiO$_2$, as the insulating layer, was used as the supporting platform. Two metal electrodes, defined by either photolithography or electron beam lithography, attached to two ends of the 1-D nanostructures were used as the source and drain electrodes. Current versus source-drain voltage and current versus gate voltage are then recorded to characterize the electrical properties of the 1-D nanostructures.

For semiconducting materials, they show either n-type behavior or p-type behavior. So there are two typical nanoscale FETs, namely, the n-channel FET and the
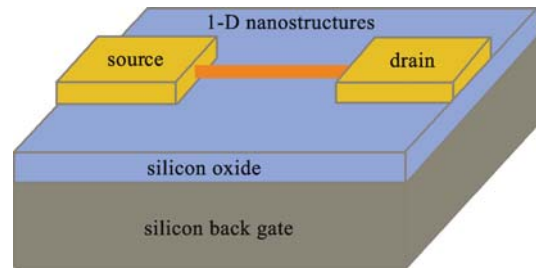

Fig. 8　Schematic of a single 1-D nanostructure-based FET

p-channel FET, respectively. For typical n-channel FET, an increase in conductance for $V_g > 0$ and a decrease in conductance for $V_g < 0$ are obtained. The p-channel FET just shows reverse electrical behavior. The capacitance of 1-D nanostructure-based FET can be calculated by using

$$C \cong 2\pi\varepsilon\varepsilon_0 L / \ln(2h/r),$$

where ε is the effective gate oxide dielectric constant, h is the thickness of the SiO$_2$ layer, L is the length of the 1-D nanostructures, and r is the radius of the 1-D nanostructures. We are also able to calculate the device mobility by using

$$\mathrm{d}I/\mathrm{d}V_g = \mu(C/L^2)V_{sd},$$

where μ is the carrier mobility [69].

There are two ways to improve the device mobility. One is to form 1-D hetero-nanowires, and the other is to dope the 1-D nanostructures with proper dopants. For example, the mobility of FET built on Ge/Si hetero-nanowires shows a device mobility of 730 cm$^2 \cdot$V$^{-1} \cdot$s^{-1}, which is more than a factor of ten greater than pure Si nanowire FET device [70]. By doping In$_2$O$_3$ nanowires with arsenic, the FET device shows a device mobility of around 1500 cm$^2 \cdot$V$^{-1} \cdot$s^{-1}, which is much higher than the best device mobility from pure In$_2$O$_3$ nanowires (514 cm$^2 \cdot$V$^{-1} \cdot$s^{-1}) [71].

The FETs built on 1-D nanostructures are able to be used as building blocks to fabricate integrated devices. For example, integrated cross nanowire p-n junctions, nanowire logic circuits were reported by using different 1-D nanostructures [17].

3.2　p-n diodes and photodetectors

The ability to fabricate high-performance n- and p-type FETs opens up the possibility of creating complex functional electronic and optoelectronic devices by forming junctions between two or more 1-D nanostructures. The p-n junction photodiodes is an alternative form of photoconductor with shorter response time and higher on/off ratio than those without the junctions [72,73]. Lieber and his co-workers fabricated nanoscale p-n diodes consisting of crossed silicon-cadmium sulfide (CdS)

nanowires as shown in Fig. 9(a) inset [72]. The *I-V* characteristic shown in Fig. 9(a) shows a sharp increase in $|I_{dark}|$ at approximately -9 V. Illuminating the device with 500 nW of 488-nm light shows a voltage-dependent photocurrent that increases with increased reverse bias. The diode has much higher sensitivity with detection limits of less than 100 photons and subwavelength spatial resolution of at least 250 nm.
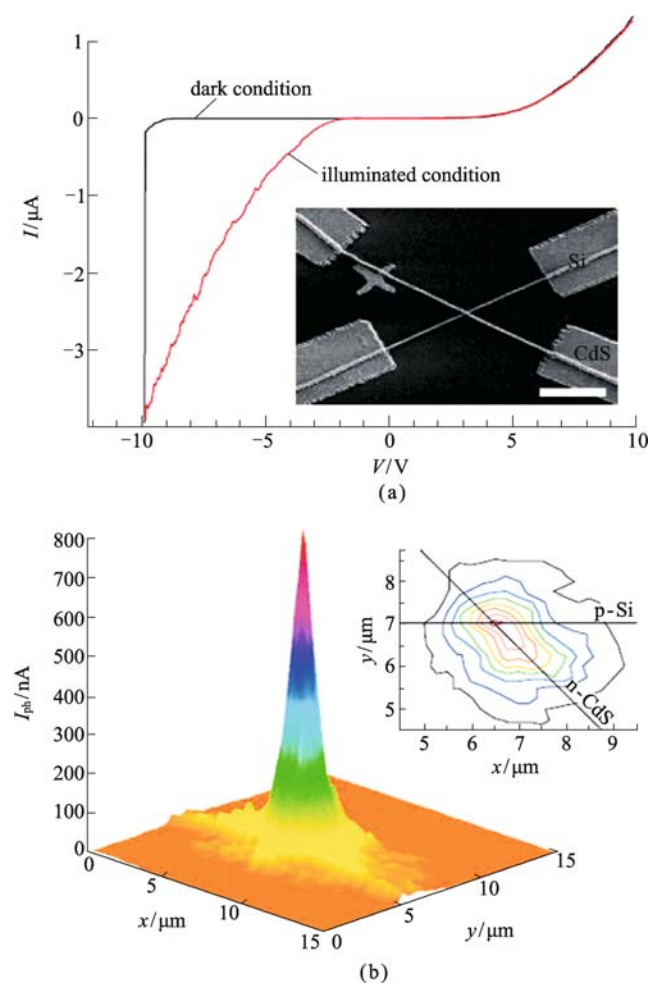

Fig. 9 (a) *I-V* characteristic of Si/CdS p-n diode in dark (black line) and illuminated (red line) conditions; (b) plot of spatially resolved photocurrent from diode measured in proportional mode using diffraction-limited laser (inset shows a contour plot with slices taken every 100 nA) (Reprinted with permission from Ref. [72])

Wang et al. fabricated a p-n photodiode by using n-type ZnO nanowires and p-type Zn_3P_2 nanowires, which were synthesized from CVD methods. The photodiode also shows rapid optical response and very high on/off ratio upon the illumination of light [73].

Individual 1-D nanostructures can be assembled into nanoscale photodetectors, and Fig. 10 shows the results from a single InP nanowire photodetector [74]. The device
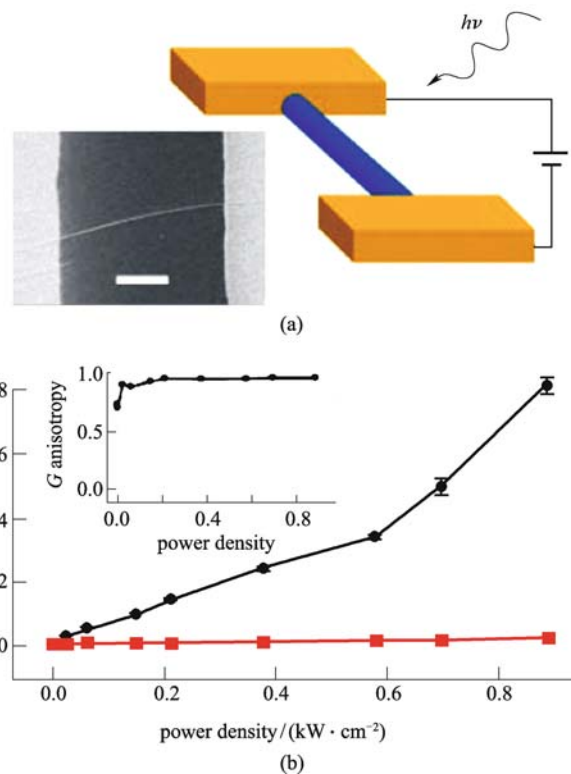

Fig. 10 Nanoscale photodetector built on a single InP nanowire. (a) Schematic diagram of nanowire photodetector; (b) conductance versus excitation power density (Reprinted with permission from Ref. [74])

structure is shown in Fig. 10(a). InP nanowires were first fabricated into FETs; then the FETs were placed in the epifluorescence microscope, and the change in conductance of the nanowire was measured via lock-in technique as a function of the laser intensity and polarization. The conductance of the device was increased by two or three orders of magnitude (Fig. 10(b)) with increasing excitation power density. Photodetectors built on 1-D nanostructures usually show very high photocurrent immediate decay ratio and fast time response.

3.3 Light-emitting diodes (LEDs)

The observation of strong photoluminescence from individual 1-D nanostructures has simulated further interest in exploiting such nanostructures for optoelectronics. Lieber and his co-workers fabricated gallium nitride-based nanowire radial heterostructures and then applied them in nanophotonics [75]. Figure 11(a) inset shows a SEM image of a nanowire LED device, in which a single n-GaN/InGaN/p-GaN core/shell/shell nanowire was used as the active material. Current versus voltage data recorded between contacts to the n-type core and p-type shell shows current rectification with a sharp onset at ca. 4 V in forward bias that is a characteristic of a p-n diode

(Fig. 11(a)). The electroluminescence (EL) spectrum collected on the nanowire device (Fig. 11(b)) exhibits an intense emission peak at 456 nm with an FWHM of 50 nm. By fine-tuning the experimental conditions, core/multishell nanowires were also produced, which were used to fabricate multicolor, high-efficiency LEDs [76]. Figure 11(c) shows the EL images collected from core/multishell nanowire LEDs with different indium compositions ranging from 1% to 40%. High brightness and systematic red shifts in emission peak were observed with the increase of indium composition.
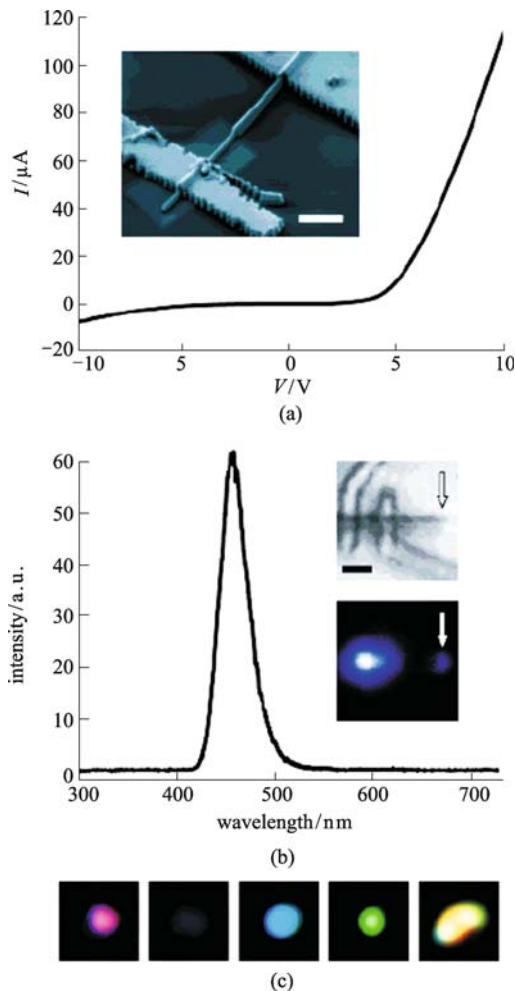
attracted great attention recently due to their potential applications in integrated photonics, sensing, and photochemotherapy [77–79]. Xu et al. reported the resonant two-photon absorption (TPA)-induced lasing performance of ZnO nanowires, and the results are shown in Fig. 12 [80]. The emission spectra of two-photon pumped ZnO nanowires for the excitation fluence of $100\,\mu J/cm^2$, $160\,\mu J/cm^2$, and $215\,\mu J/cm^2$ were shown in Fig. 12(a). The integrated emission intensities as functions of the excitation fluence for ZnO nanowires pumped in one-photon absorption (OPA) and TPA regimes were shown in Fig. 12(b). It can be seen that a remarkably low threshold of $160\,\mu J/cm^2$ was observed for the TPA-induced laser actions.

Miniaturized multicolour lasers could be enabled with the development of a tunable band-gap nanoscale gain

Fig. 11 (a) Current (I) versus voltage (V) curve recorded on n-GaN/InGaN/p-GaN core/shell/shell nanowire; (b) electroluminescence (EL) spectrum recorded from forward-biased core/shell/shell p-n junction at 7 V (insets: bright field (upper) and EL (lower) image of the structure); (c) optical microscopy images collected from core/multishell nanowire LEDs in forward bias, showing purple, blue, greenish-blue, green, and yellow emission, respectively (Reprinted with permission from Ref. [75])

3.4 Nanolasers

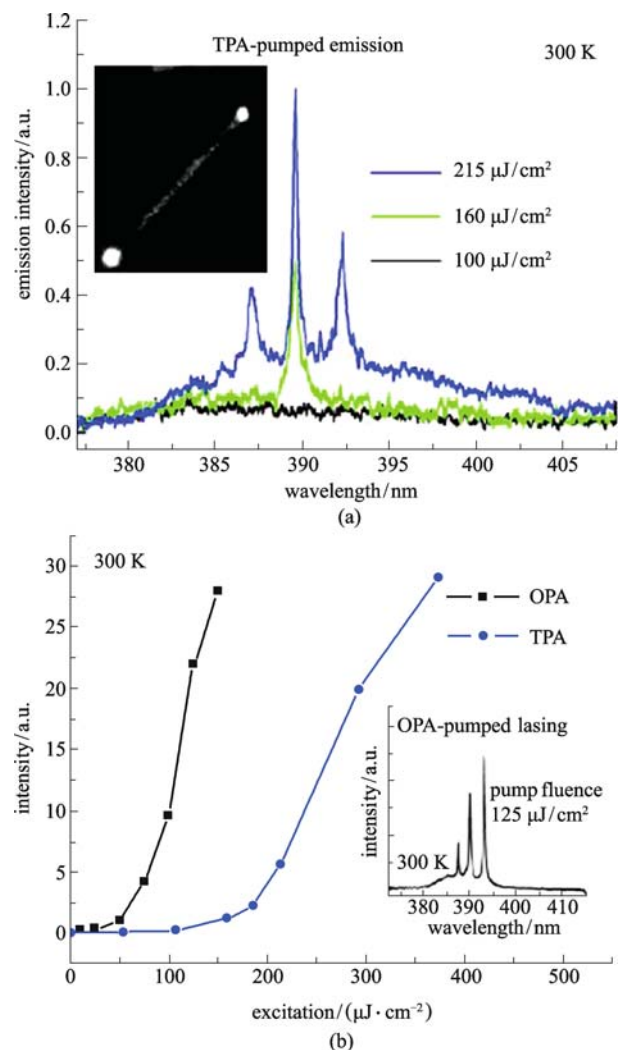Nanoscale UV lasers based on 1-D nanostructures have

Fig. 12 (a) Two-photon pumped emission spectra from ZnO nanowires for different excitation fluence; (b) integrated emission intensity from ZnO nanorods pumped by one-photon and two-photon processes versus excitation fluence (Reprinted with permission from Ref. [80])

medium that is coupled effectively into a small optical cavity. Lieber et al. reported the use of multi-quantum-well nanowire heterostructures as wavelength-controlled lasers [81]. The used nanowire heterostructures were GaN nanowire cores covered with composition-tunable InGaN/GaN multi-quantum-well shells, which served as the composition-tunable gain medium. Figure 13 shows the photoluminescence images and normalized photoluminescence spectra recorded from the multi-quantum-well nanowire heterostructures with different compositions. These nanolasers showed composition-dependent emission from 365 to 494 nm, and the threshold is reduced for an increasing n-value. These nanostructures are expected to yield free-standing injection nanolasers.

3.5   Single nanowire solar cells

Solar energy conversion devices like solar cells provide direct resolutions to solve the continuously increasing energy problems. 1-D nanostructures can be used to fabricate high-performance solar cells. Yang et al. fabricated several dye-sensitized solar cells (DSSCs) using arrays of core/shell ZnO/Al_2O_3, ZnO/TiO_2 nanowires and solar cells using n/p core/shell Si nanowires [82–86].

A breakthrough work on 1-D nanostructure-based solar cells was done by Lieber et al. in 2007 [87]. They developed the first single-nanowire-based solar cells using core/shell p-i-n silicon nanowires, which were synthesized by a nanocluster-catalyzed vapor-liquid-solid method. Typical nanowire has a diameter of around 300 nm. Figures 14(a) and 14(b) show the schematics and corresponding SEM images of the device fabrication process. Figure 14(c) shows the dark and light I-V curves

recorded from a single solar cell. It can be seen that a single solar cell yields an open-circuit voltage of 0.260 V, a short-circuit current of 0.503 nA and a fill factor of 55.0%. Careful studies reveal that a single solar cell device yields a maximum power output of up to 200 pW and an apparent energy conversion efficiency of ~3.4% under solar equivalent illumination. The single-nanowire solar cells can be used to power tiny sensors for environmental monitoring applications. For example, Fig. 14(d) shows the real-time detection of the voltage drop across a p-type silicon nanowire sensor under different pH values. The sensor was powered by the single-nanowire solar cell, which showed a very good stability.

In the following work, the same group developed photovoltaics by using coaxial group III nitride nanowires as well as single and tandem axial p-i-n nanowire photovoltaic devices [88,89]. Though the efficiencies of these nanowire solar cell devices are relatively lower than conventional solar cells, it is believed that efficiencies can be greatly improved with optimized experimental procedures or by developing new 1-D nanostructures.

3.6   Chemical and biosensors

With large surface-to-volume ratios and a Debye length comparable to their dimensions, 1-D nanostructures have showed great potentials to be used as chemical sensors or biosensors. There are several types of sensors built on 1-D nanostructures, such as chemoresistors, FET-based sensors, and alternating current (AC) impedance sensors [90–95]. Among these three types, the FET-based sensors are the most important ones that have been extensively investigated. The sensing mechanism mainly relies on the change of electrical conductivity contributed by
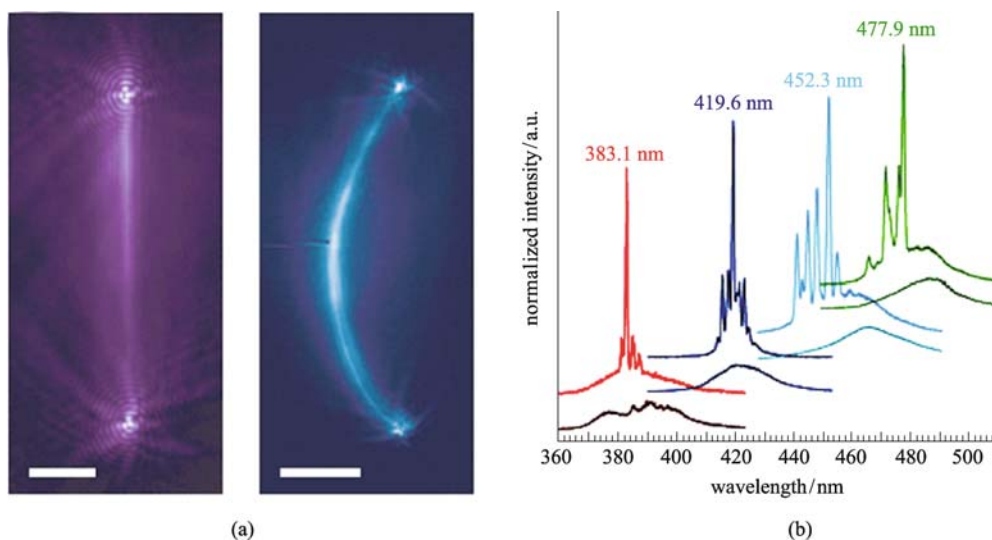

Fig. 13   (a) Photoluminescence images recorded from $GaN/In_{0.05}Ga_{0.95}N$ and $GaN/In_{0.23}Ga_{0.77}N$ multi-quantum-well nanowire structures; (b) normalized photoluminescence spectra collected from four representative 26 multi-quantum-well nanowire structures with increasing In composition pumped at ~250 and ~700 kW·cm^{-2}, respectively (Reprinted with permission from Ref. [81])
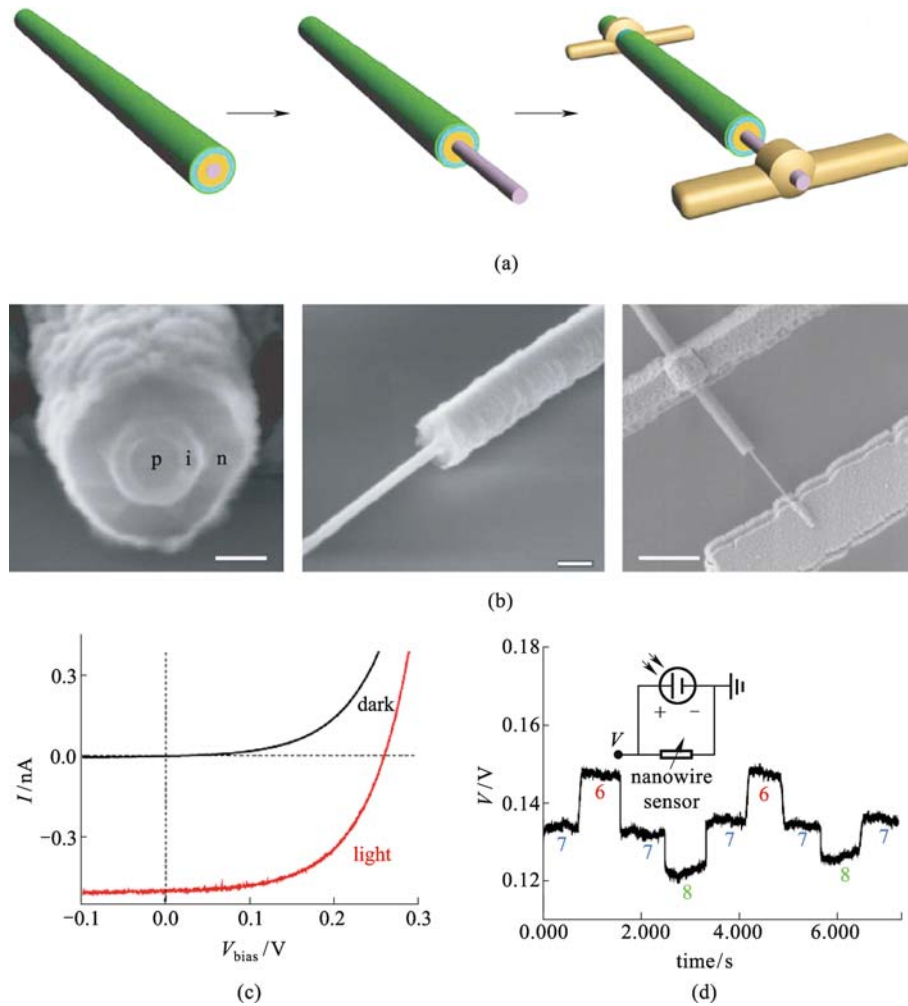
Fig. 14 (a) Schematics of single-nanowire-based solar cell fabrication; (b) SEM images corresponding to schematics shown in (a); (c) dark and light *I-V* curves; (d) real-time detection of voltage drop across aminopropyltriethoxysilane-modified silicon nanowire at different pH values, which is powered by a single nanowire solar cell (Reprinted with permission from Ref. [87])

interactions between 1-D nanostructures and the surrounding environment.

Zhou et al. reported the first single In_2O_3 nanowire-FET-based chemical sensors [90]. Figure 15(a) shows the *I-V* curves recorded from a chemical sensor before and after exposing the FET to 100 ppm NO_2 in Ar for 5 min with 0 V applied to the silicon gate electrode. The change in device conductance was clearly seen from the *I-V* curves. After exposure, the device was easily recovered to its initial status within a short time by pumping down the system to vacuum followed by UV illumination to desorb the attached NO_2 molecules. Figure 15(b) shows the *I-V* curves recorded from the device before and after exposure to 1% NH_3. A reduction in device conductance of five orders of magnitude was obtained after exposing to the gases, also revealing good sensitivity. The sensitivities, such as detection limit and sensing time, of FET-based chemical sensors can be easily improved by forming nanowire thin-film sensors. For example, Zhou et al.

fabricated chemical sensors using In_2O_3 nanowire networks as the sensing elements. This kind of nanowire thin-film sensors shows much lower detection limit of 5 ppb NO_2 than the single-nanowire sensors of 20 ppb NO_2 [91].

Integrating several kinds of 1-D nanostructures into a single sensor, the so-called electronic nose, makes it possible to detect different chemicals. Zhou et al. fabricated such electronic nose using four different kinds of nanowires, including carbon nanotubes, ZnO nanowires, SnO_2 nanowires, and In_2O_3 nanowires, as the sensing elements based on a micromachined hot plate technique developed by the same group [94,95]. Such electronic nose can be used to selectively detect gases like NO_2, H_2, ethanol, and others.

Recently, Wang et al. developed a very interesting Schottky-gated nanowire chemical and biosensors [96]. This kind of sensors has several unique features like much-enhanced sensitivity and very short sensing time,
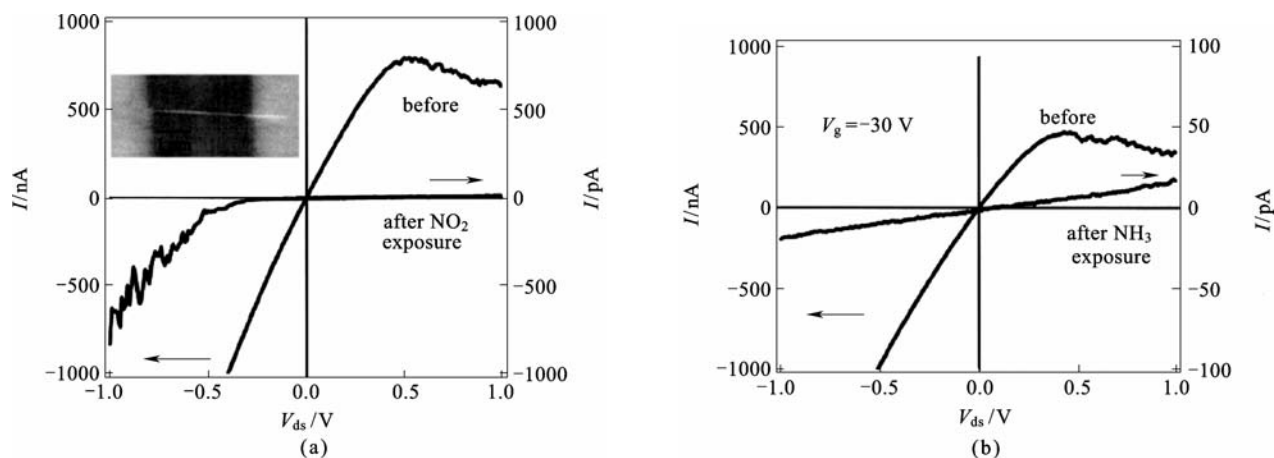
Fig. 15 (a) I-V curves measured before and after exposure to 100 ppm NO$_2$ gases; (b) I-V curves measured before and after exposure to 1% NH$_3$ (Reprinted with permission from Ref. [90])

compared with the conventional nanowire sensors. For instance, they deliberately introduced a nonsymmetrical Schottky contact at one end of a ZnO nanowire sensor to detect molecules like hemoglobin. A low detection limit of 2 fg/mL was obtained on the biosensor.

3.7 Nanogenerators

Energy harvesting from the ambient environment is an active research field of nanotechnology nowadays. 1-D nanostructures were found to be able to fabricate into interesting nanogenerators, developed by Wang's group in Georgia Institute of Technology, and can be used to drive small nanodevices [97–106]. The concept of the nanogenerators was first introduced by examining the piezoelectric properties of ZnO nanowires with an atomic force microscopy (AFM). Figure 16(a) is the SEM image of aligned ZnO nanowires grown on a conductive solid
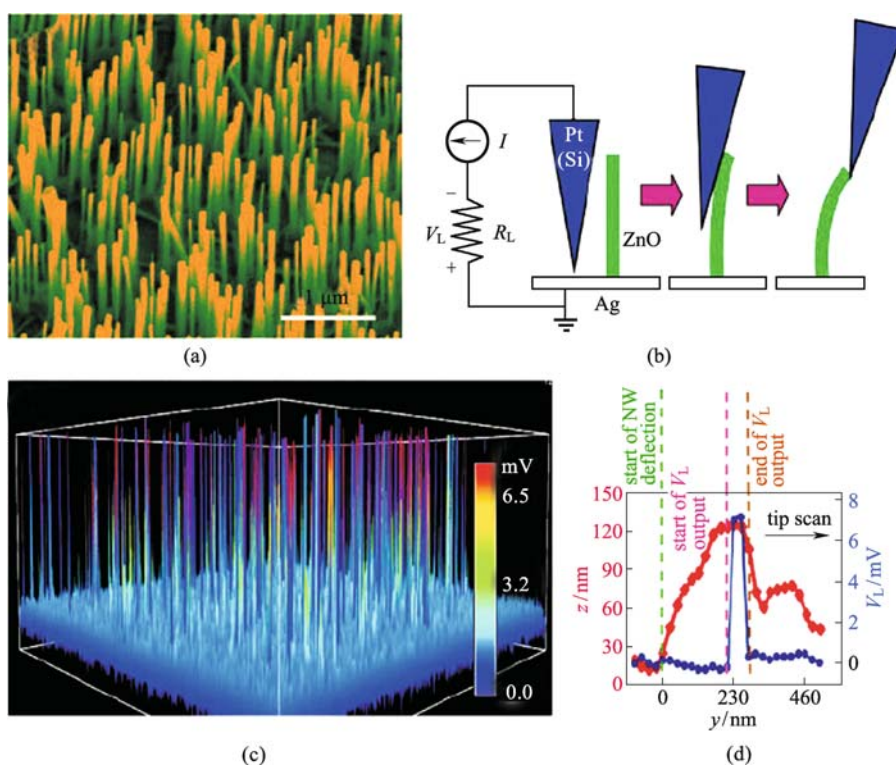

Fig. 16 (a) SEM image of aligned ZnO nanowires; (b) experimental setup and procedure for generating electricity using conductive AFM tip; (c) output-voltage image of nanowire arrays when AFM tip scans across them; (d) overlap plot of AFM topological image and corresponding generated voltage for a single scan of tip across nanowire (Reprinted with permission from Ref. [106])

substrate by using a CVD method. Integrating the material into an AFM, a Si AFM tip coated with Pt film was used to measure the device (Fig. 16(b)) in a contact mode. Figure 16(c) shows the output-voltage image obtained on the ZnO nanowire arrays. Many sharp output peaks were observed. Figure 16(d) is the topological profile of a ZnO nanowire and its corresponding output potential. A delay was observed for the voltage output signal. The delay is a key signature of the power-output process.

Following this work, Wang et al. developed several kinds of nanogenerators, such as piezoelectric FETs, nanoforce sensors, and gate diodes.

4   Conclusions and remarks

In conclusion, we provide a comprehensive review of the state-of-the-art research activities focusing on nanoscale electronic and optoelectronic devices using 1-D nano-structures as the device elements. Both the synthesis and device applications of 1-D nanostructures are reviewed in the paper in order to give the readers a clear map of this interesting research topic. We believe that the fascinating achievements in this top should inspire more and more research efforts to address the remaining challenges.

Though a lot of research works have been done in the research topic of device applications of 1-D nanostructures, there is still plenty of room for scientific, engineering, and technological researches. First, precise control of the dimension, composition, doping state, and morphology of 1-D nanostructures still needs a lot of research efforts since the device performance is largely dependent on these parameters. After synthesis, the physical properties of 1-D nanostructures should be studied more in detail towards a full understanding of the growth mechanism and the relationship between structure and the properties. Further-more, developing new device concepts, structures, and their integration will be essential to make full use of 1-D nanostructures. On the other hand, the assembly of 1-D nanostructures, though not mentioned in the article, should be paid more attention since it is the central technique for device integration and their future real applications.

References

1. Wang Z L. Nanowires and Nanobelts: Materials, Properties and Devices. Netherlands: Kluwer Academic Publishers, 2003

2. Li Y, Qian F, Xiang J, Lieber C M. Nanowire electronic and optoelectronic devices. Materials Today, 2006, 9(10): 18–27

3. Meindl J D, Chen Q, Davis J A. Limits on silicon nanoelectronics for terascale integration. Science, 2001, 293(5537): 2044–2049

4. Shen G Z, Chen D, Chen P C, Zhou C. Vapor-solid growth of one-dimensional layer-structured gallium sulfide nanostructures. ACS Nano, 2009, 3(5): 1115–1120

5. Chen P C, Shen G Z, Zhou C. Chemical sensors and electronic noses based on 1-D metal oxide nanostructures. IEEE Transactions on Nanotechnology, 2008, 7(6): 668–682

6. Zhang J, Chen P C, Shen G Z, He J B, Kumbhar A, Zhou C, Fang J. P-type field-effect transistors of single-crystal zinc telluride nanobelts. Angewandte Chemie—International Edition, 2008, 47(49): 9469–9471

7. Shen G Z, Chen D. Self-coiling of $Ag_2V_4O_{11}$ nanobelts into perfect nanorings and microloops. Journal of the American Chemical Society, 2006, 128(36): 11762–11763

8. Duan X, Huang Y, Cui Y, Wang J, Lieber C M. Indium phosphide nanowires as building blocks for nanoscale electronic and optoelectronic devices. Nature, 2001, 409(6816): 66–69

9. Huang Y, Duan X, Wei Q, Lieber C M. Directed assembly of one-dimensional nanostructures into functional networks. Science, 2001, 291(5504): 630–633

10. Shen G Z, Chen D, Zhou C. One-step thermo-chemical synthetic method for nanoscale one-dimensional heterostructures. Chemistry of Materials, 2008, 20(12): 3788–3790

11. Pan Z W, Dai Z R, Wang Z L. Nanobelts of semiconducting oxides. Science, 2001, 291(5510): 1947–1949

12. Dai Z R, Pan Z W, Wang Z L. Gallium oxide nanoribbons and nanosheets. Journal of Physical Chemistry B, 2002, 106(5): 902–904

13. Comini E, Faglia G, Sberveglieri G, Pan Z W, Wang Z L. Stable and highly sensitive gas sensors based on semiconducting oxide nanobelts. Applied Physics Letters, 2002, 81(10): 1869–1871

14. Shen G Z, Chen D, Lee C J. Hierarchical saw-like ZnO nanobelt/ZnS nanowire heterostructures induced by polar surfaces. Journal of Physical Chemistry B, 2006, 110(32): 15689–15693

15. Shen G Z, Bando Y, Chen D, Liu B D, Zhi C Y, Golberg D. Morphology-controlled growth of ZnO nanostructures by a round-to-round metal vapor deposition method. Journal of Physical Chemistry B, 2006, 110(9): 3973–3978

16. Cui Y, Wei Q, Park H, Lieber C M. Nanowire nanosensors for highly sensitive and selective detection of biological and chemical species. Science, 2001, 293(5533): 1289–1292

17. Huang Y, Duan X, Cui Y, Lauhon L J, Kim K, Lieber C M. Logic gates and computation from assembled nanowire building blocks. Science, 2001, 294(5545): 1313–1317

18. Shen G Z, Bando Y, Hu J Q, Golberg D. High-symmetry ZnS hepta- and tetrapods composed of assembled ZnS nanowire arrays. Applied Physics Letters, 2007, 90(12): 123101

19. Law M, Kind H, Messer B, Kim F, Yang P. Photochemical sensing of NO_2 with SnO_2 nanoribbon nanosensors at room temperature. Angewandte Chemie—International Edition, 2002, 41(13): 2405–2408

20. Kolmakov A. Chemical sensing and catalysis by one-dimensional nanostructures. International Journal of Nanotechnology, 2008, 5(4–5): 450–474

21. Shen G Z, Bando Y, Golberg D. Self-assembled hierarchical

single-crystalline β-SiC nanoarchitectures. Crystal Growth & Design, 2007, 7(1): 35–38

22. Dai Z R, Pan Z W, Wang Z L. Novel nanostructures of functional oxides synthesized by thermal evaporation. Advanced Functional Materials, 2003, 13(1): 9–24

23. Arnold M S, Avouris P, Pan Z W, Wang Z L. Field-effect transistors based on single semiconducting oxide nanobelts. Journal of Physical Chemistry B, 2003, 107(3): 659–663

24. Wang Z L. Functional oxide nanobelts: materials, properties and potential applications in nanosystems and biotechnology. Annual Review of Physical Chemistry, 2004, 55: 159–196

25. Shen G Z, Bando Y, Ye C H, Yuan X L, Sekiguchi T, Golberg D. Single-crystal nanotubes of II$_3$-V$_2$ semiconductors. Angewandte Chemie—International Edition, 2006, 45(45): 7568–7572

26. Duan X, Huang Y, Agarwal R, Lieber C M. Single-nanowire electrically driven lasers. Nature, 2003, 421(6920): 241–245

27. Zhong Z, Qian F, Wang D, Lieber C M. Synthesis of p-type gallium nitride nanowires for electronic and photonic nanodevices. Nano Letters, 2003, 3(3): 343–346

28. Zhong Z, Wang D, Cui Y, Bockrath M W, Lieber C M. Nanowire crossbar arrays as address decoders for integrated nanosystems. Science, 2003, 302(5649): 1377–1379

29. Shen G Z, Bando Y, Liu B D, Tang C C, Golberg D. Unconventional zigzag indium phosphide single-crystalline and twinned nanowires. Journal of Physical Chemistry B, 2006, 110 (41): 20129–20132

30. Wang Z L, Kong X Y, Ding Y, Gao P X, Hughes W L, Yang R S, Zhang Y. Semiconducting and piezoelectric oxide nanostructures induced by polar surfaces. Advanced Functional Materials, 2004, 14(10): 943–956

31. Huang M, Choudrey A, Yang P. Ag nanowire formation within mesoporous silica. Chemical Communications, 2002, 12: 1063–1064

32. Shen G Z, Bando Y, Liu B D, Tang C C, Huang Q, Golberg D. Systematic investigation of the formation of 1D α-Si$_3$N$_4$ nanostructures by using a thermal-decompsition/nitridation process. Chemistry—A European Journal, 2006, 12(11): 2987–2993

33. Shen G Z, Bando Y, Golberg D. Self-assembled three-dimensional structures of single-crystalline ZnS submicrotubes formed by coalescence of ZnS nanowires. Applied Physics Letters, 2006, 88 (12): 123107

34. Gudiksen M S, Lauhon L J, Wang J, Smith D, Lieber C M. Growth of nanowire superlattice structures for nanoscale photonics and electronics. Nature, 2002, 415(6872): 617–620

35. Duan X, Huang Y, Cui Y, Lieber C M. Nonvolatile memory and programmable logic from molecule-gated nanowires. Nano Letters, 2002, 2(5): 487–490

36. Shen G Z, Chen D, Bando Y, Golberg D. One-dimensional (1-D) nanoscale heterostructures. Journal of Materials Science & Technology, 2008, 24(4): 541–549

37. Qiu X F, Lou Y B, Samia A C S, Devadoss A, Burgess J D, Dayal S, Burda C. PbTe nanorods by sonoelectronchemistry. Angewandte Chemie—International Edition, 2005, 44(36): 5855–5857

38. Shen G Z, Bando Y, Tang C C, Golberg D. Self-organized hierarchical ZnS/SiO$_2$ nanowire heterostructures. Journal of Physical Chemistry B, 2006, 110(14): 7199–7202

39. Wang D, Qian F, Yang C, Zhong Z, Lieber C M. Rational growth of branched and hyperbranched nanowire structures. Nano Letters, 2004, 4(5): 871–874

40. Jin S, Whang D, McAlpine M C, Friedman R S, Wu Y, Lieber C M. Scalable interconnection and integration of nanowire devices without registration. Nano Letters, 2004, 4(5): 915–919

41. Lauhon L J, Gudiksen M S, Lieber C M. Semiconductor nanowire heterostructures. Philosophical Transactions of the Royal Society of London A, 2004, 362: 1247–1260

42. Shen G Z, Chen D. One-dimensional nanostructures and devices of II-V group semiconductors. Nanoscale Research Letters, 2009, 4 (8): 779–788

43. Yu G, Li X, Lieber C M, Cao A. Nanomaterial-incorporated blown bubble films for large-area, aligned nanostructures. Journal of Materials Chemistry, 2008, 18(7): 728–734

44. Lu W, Lieber C M. Nanoelectronics from the bottom up. Nature Materials, 2007, 6(11): 841–850

45. Hu Y, Churchill H O H, Reilly D J, Xiang J, Lieber C M, Marcus C M. A Ge/Si heterostructure nanowire-based double quantum dot with intetrated charge sensor. Nature Nanotechnology, 2007, 2(10): 622–625

46. Patolsky F, Timko B P, Zheng G, Lieber C M. Nanowire-based nanoelectronic devices in the life science. MRS Bulletin, 2007, 32 (22): 142–149

47. Shen G Z, Chen P C, Ryu K, Zhou C. Devices and chemical sensing applications of metal oxide nanowires. Journal of Materials Chemistry, 2009, 19(7): 828–839

48. Li C, Zhang D, Han S, Liu X, Tang T, Zhou C. Diameter-controlled growth of single-crystalline In$_2$O$_3$ nanowires and their electronic properties. Advanced Materials, 2003, 15(2): 143–146

49. Ju S, Li J, Liu J, Chen P C, Ha Y, Ishikawa F N, Chang H K, Zhou C, Facchetti A, Janes D B, Marks T J. Transparent active matrix organic light-emitting diode displays driven by nanowire transistor circuitry. Nano Letters, 2008, 8(4): 997–1004

50. Melosh N A, Boukai A, Diana F, Gerardot B, Badolato A, Petroff P M, Heath J R. Ultrahigh-density nanowire lattices and circuits. Science, 2003, 300(5616): 112–115

51. Huang M H, Mao S, Feick H, Yan H, Wu Y, Kind H, Weber E, Russo R, Yang P. Room-temperature ultraviolet nanowire nanolasers. Science, 2001, 292(5523): 1897–1899

52. Cao G Z, Liu D W. Template-based synthesis of nanorod, nanowire, and nanotube arrays. Advanced Colloid Interface Science, 2008, 136(1–2): 45–64

53. Rao C N R, Deepak F L, Gundiah G, Govindaraja A. Inorganic nanowires. Progress in Solid State Chemistry, 2003, 31(1–2): 5–147

54. Ming T, Kou X S, Chen H J, Wang T, Tam H L, Cheah K W, Chen J Y, Wang J F. Angewandte Chemie—International Edition, 2008, 47(50): 9685–9690

55. Kim S, Kim S K, Park S. Bimetallic gold-silver nanorods produce multiple surface plasmon bands. Journal of the American Chemical Society, 2009, 131(24): 8380–8381

56. Khanal B P, Zubarev E R. Purification of high aspect ratio gold nanorods: complete removal of platelets. Journal of the American Chemical Society, 2008, 130(38): 12634–12635

57. Iijima S. Helical microtubules of graphitic carbon. Nature, 1991,

354(6348): 56–58

58. Shen G Z, Bando Y, Golberg D. Recent developments in single-crystal inorganic nanotubes synthesized from removable templates. International Journal of Nanotechnology, 2007, 4(6): 730–749

59. Shen G Z, Bando Y, Golberg D. Size-tunable synthesis of SiO₂ nanotubes via a simple *in situ* templatelike process. Journal of Physical Chemistry B, 2006, 110(46): 23170–23174

60. Shen G Z, Bando Y, Zhi C Y, Golberg D. Tubular carbon nano/microstructures synthesized from graphite powders by an *in situ* template process. Journal of Physical Chemistry B, 2006, 110(22): 10714–10719

61. Gautam U K, Vivekchand S R C, Govindaraj A, Kulkarni G U, Selvi N R, Rao C N R. Generation of onions and nanotubes of GaS and GaSe through laser and thermally induced exfoliation. Journal of the American Chemical Society, 2005, 127(1111): 3658–3659

62. Goldberger J, He R R, Zhang Y F, Lee S W, Yan H, Choi H J, Yang P. Single-crystal gallium nitride nanotubes. Nature, 2003, 422 (6932): 599–602

63. Fan H J, Yang Y, Zacharias M. ZnO-based ternary compound nanotubes and nanowires. Journal of Materials Chemistry, 2009, 19(7): 885–900

64. Yu Q J, Fu W, Yu C, Yang H, Wei R, Li M, Liu S, Sui Y, Liu Z, Yuan M, Zou G, Wang G, Shao C, Liu Y. Fabrication and optical properties of large-scale ZnO nanotube bundles via a simple solution route. Journal of Physical Chemistry C, 2007, 111(47): 17521–17526

65. Fan H J, Gosele U, Zacharias M. Formation of nanotubes and hollow nanoparticles based on Kirkendall and diffusion processes: a review. Small, 2007, 3(10): 1660–1671

66. Shen G Z, Bando Y, Golberg D. Synthesis and structures of high-quality single-crystalline II₃-V₂ semiconductor nanobelts. Journal of Physical Chemistry C, 2007, 111(13): 5044–5049

67. Shen G Z, Cho J H, Yoo J K, Yi G C, Lee C J. Synthesis of single-crystal CdS microbelts using a modified thermal evaporation method and their photoluminescence. Journal of Physical Chemistry B, 2005, 109(19): 9294–9298

68. Choi J R, Oh S J, Ju H, Cheon J. Massive fabrication of free-standing one-dimensional Co/Pt nanostructures and modulation of ferromagnetism via a programmable barcode layer effect. Nano Letters, 2005, 5(11): 2179–2183

69. Huang Y, Duan X F, Lieber C M. Semiconductor Nanowires: Nanoscale Electronics and Optoelectronics. London: Taylor & Francis, 2005

70. Xiang J, Lu W, Hu Y, Wu Y, Yan H, Lieber C M. Ge/Si nanowire heterostructures as high-performance field-effect transistors. Nature, 2006, 441(7092): 489–493

71. Chen P C, Shen G Z, Chen H, Ha Y G, Wu C, Sukcharoenchoke S, Fu Y, Liu J, Facchetti A, Marks T J, Thompson M E, Zhou C. High-performance single-crystalline arsenic-doped indium oxide nanowires for transparent thin-film transistors and active matrix organic light-emitting diode displays. ACS Nano, 2009, 3(11): 3383–3390

72. Hayden O, Agarwal R, Lieber C M. Nanoscale avalanche photodiodes for highly sensitive and spatially resolved photon detection. Nature Materials, 2006, 5(5): 352–356

73. Yang R, Chueh Y L, Morber J R, Snyder R, Chou L J, Wang Z L. Single-crystalline branched zinc phosphide nanostructures: synthesis, properties, and optoelectronic devices. Nano Letters, 2007, 7 (2): 269–275

74. Wang J, Gudiksen M S, Duan X, Cui Y, Lieber C M. Highly polarized photoluminescence and photodetection from single indium phosphide nanowires. Science, 2001, 293(5534): 1455–1457

75. Qian F, Li Y, Gradecak S, Wang D, Barrelet C J, Lieber C M. Gallium nitride-based nanowire radial heterostructures for nano-photonics. Nano Letters, 2004, 4(10): 1975–1979

76. Qian F, Gradecak S, Li Y, Wen C Y, Lieber C M. Core/multishell nanowire heterostructures as multicolor, high-efficiency light-emitting diodes. Nano Letter, 2005, 5(11): 2287–2291

77. Johnson J C, Yan H, Schaller R D, Haber L H, Saykally R J, Yang P. Single nanowire lasers. Journal of Physical Chemistry B, 2001, 105(46): 11387–11390

78. Yan H, He R, Johnson J, Law M, Saykally R J, Yang P. Dendrite nanowire UV laser array. Journal of the American Chemical Society, 2003, 125(16): 4728–4729

79. Yan H, Justin J, Law M, Saykally R, Yang P. Nanoribbon UV lasers. Advanced Materials, 2003, 15(6): 1907–1911

80. Zhang C, Zhang F, Xia T, Kumar N, Hahm J I, Liu J, Wang Z L, Xu J. Low-threshold two-photon pumped ZnO nanowire lasers. Optics Express, 2009, 17(10): 7894–7900

81. Qian F, Li Y, Gradecak S, Park H G, Dong Y, Ding Y, Wang Z L, Lieber C M. Multi-quantum-well nanowire heterostructures for wavelength-controlled lasers. Nature Materials, 2008, 7(9): 701–706

82. Law M, Greene L E, Johnson J C, Saykally R, Yang P. Nanowire dye-sensitized solar cells. Nature Materials, 2005, 4(6): 455–459

83. Law M, Greene L E, Radenovic A, Kuykendall T, Liphardt J, Yang P. Core-shell nanowire dye-sensitized solar cells. Journal of Physical Chemistry B, 2006, 110(45): 22652–22663

84. Greene L E, Law M, Yuhas B D, Yang P. ZnO-TiO₂ core/shell nanorod/P3HT solar cells. Journal of Physical Chemistry C, 2007, 111(50): 18451–18456

85. Garnett E C, Yang P. Silicon nanowire radial p-n junction solar cells. Journal of the American Chemical Society, 2008, 130(29): 9224–9225

86. Yuhas B, Yang P. Nanowire-based all-oxide solar cell. Journal of the American Chemical Society, 2009, 131(12): 3756–3757

87. Tian B, Zheng X, Kempa T J, Fang Y, Yu N, Yu G, Huang J, Lieber C M. Coaxial silicon nanowires as solar cells and nanoelectronic power sources. Nature, 2007, 449(7164): 885–889

88. Dong Y, Tian B, Kempa T, Lieber C M. Coaxial group III-nitride nanowire photovoltaics. Nano Letters, 2009, 9(5): 2183–2187

89. Kempa T J, Tian B, Kim D R, Hu J, Zheng X, Lieber C M. Single and tandem axial p-i-n nanowire photovoltaic devices. Nano letters, 2008, 8(10): 3456–3460

90. Li C, Zhang D, Liu X, Han S, Tang T, Han J, Zhou C. In₂O₃ nanowires as chemical sensors. Applied Physics Letters, 2003, 82 (10): 1613–1615

91. Zhang D, Liu Z, Li C, Tang T, Liu X, Han S, Lei B, Zhou C. Detection of NO₂ down to ppb levels using individual and multiple In₂O₃ nanowire devices. Nano Letters, 2004, 4(10): 1919–1923

92. Curreli M, Li C, Sun Y, Lei B, Gundersen M A, Thompson M E, Zhou C. Selective functionalization of In$_2$O$_3$ nanowire mat devices for biosensing application. Journal of the American Chemical Society, 2005, 127(19): 6922–6923

93. Ishikawa F N, Chang H, Curreli M, Liao H, Olson C, Chen P, Zhang R, Roberts R, Sun R, Cote R, Thompson M, Zhou C. Label-free, electrical detection of the SARS virus N-protein with nanowire biosensors utilizing antibody mimics as capture probes. ACS Nano, 2009, 3(5): 1219–1225

94. Chen P, Ishikawa F N, Chang H, Ryu K, Zhou C. Nano electronic nose: a hybrid nanowire/carbon nanotube sensor array with integrated micromachined hotplates for sensitive gas discrimination. Nanotechnology, 2009, 20(12): 125503

95. Ryu K, Zhang D, Zhou C. High-performance metal oxide nanowire chemical sensors with integrated micromachined hotplates. Applied Physics Letters, 2008, 92(9): 93111–93113

96. Yeh P H, Li Z, Wang Z L. Schottky-gated probe-free ZnO nanowire biosensor. Advanced Materials, 2009, 21(48): 4975–4978

97. Wang Z L, Song J H. Piezoelectric nanogenerators based on zinc oxide nanowire arrays. Science, 2006, 312(5771): 242–246

98. Wang X D, Zhou J, Song J H, Liu J, Xu N S, Wang Z L. Piezoelectric field effect transistor and nanoforce sensor based on a single ZnO nanowire. Nano Letters, 2006, 6(12): 2768–2772

99. Gao P, Song J, Liu J, Wang Z L. Nanowire piezoelectric nanogenerators on plastic substrates as flexible power sources for nanodevices. Advanced Materials, 2007, 19(1): 67–72

100. He J H, Hsin C L, Liu J, Chen L J, Wang Z L. Piezoelectric gated diode of a single ZnO nanowire. Advanced Materials, 2007, 19(6): 781–784

101. Wang X D, Liu J, Song J, Wang Z L. Integrated nanogenerators in biofluid. Nano Letters, 2007, 7(8): 2475–2479

102. Lin Y F, Song J, Ding Y, Liu S, Wang Z L. Piezoelectric nanogenerator using CdS nanowires. Applied Physics Letters, 2008, 92(2): 022105

103. Qin Y, Wang X, Wang Z L. Microfibre-nanowire hybrid structure for energy scavenging. Nature, 2008, 451(7180): 809–813

104. Xu S, Wei Y, Liu J, Yang R, Wang Z L. Integrated multilayer nanogenerator fabricated using paired nanotip-to-nanowire brushes. Nano Letters, 2008, 8(11): 4027–4032

105. Yang R, Qin Y, Dai L, Wang Z L. Power generation with laterally-packaged piezoelectric fine wires. Nature Nanotechnology, 2009, 4(1): 34–39

106. Wang Z L. Towards self-powered nanosystems: from nanogenerators to nanopiezotronics. Advanced Functional Materials, 2008, 18(22): 3553–3567